Synthesis of micron-sized spherical $LaPO_4$:Ce,Tb phosphor by a homogeneous precipitation method

L. M. SHAN[a,*], H. TANG[a], Z. H. LI[a], Z. Z. WANG[a], G. B. LIU[b]
[a]*Department of Material Science, Sichuan Engineering Technical College, Deyang 618000, China*
[b]*College of Materials Science and Engineering, Sichuan University, Chengdu 610064, China*

Micron-sized spherical $LaPO_4$:Ce,Tb precipitate was synthesized by a new homogeneous precipitation method. Then, spherical $LaPO_4$:Ce,Tb phosphor was fabricated using as-prepared $LaPO_4$:Ce,Tb precipitate as a precursor. The morphologies of $LaPO_4$:Ce,Tb precipitate and phosphor were detected by scanning electron microscopy (SEM). The structures of $LaPO_4$:Ce,Tb precipitate and phosphor were characterized by X-ray diffraction (XRD). Then, the growth mechanism of spherical $LaPO_4$:Ce,Tb precipitate was investigated. The results indicate that the $LaPO_4$:Ce,Tb precipitate particles were the secondary agglomerated particle of needle-shape primary nano-particles. The $LaPO_4$:Ce,Tb phosphor particles remain the same morphology of the precipitate particles. The diameters of $LaPO_4$:Ce,Tb phosphor particles are between 2.0 and 5.0 μm. Meanwhile, as-prepared spherical $LaPO_4$:Ce,Tb phosphor exhibits stronger emission intensity than irregular one fabricated by a conventional co-precipitation method, which is ascribed to a smoother surface of the dispersive spherical particles.

(Received October 5, 2014; accepted November 13, 2014)

Keyword: Morphology, Spherical phosphor, $LaPO_4$:Ce,Tb, Co-precipitation

1. Introduction

$LaPO_4$:Ce,Tb phosphor has attracted extensive attention over the last decade because of its high quantum efficiency, stability at high temperature and good matching with Y_2O_3:Eu^{3+} red phosphor. To date, different synthesis methods, such as solid-state reaction method [1, 2], hydrothermal reaction approach [3, 4], spray pyrolysis method [5, 6], sol-gel method [7–9], hydrolyzed colloid reaction technique [10–13], ionic liquid based method [14–16], co-precipitation method [17–26], have been reported to prepare $LaPO_4$:Ce,Tb phosphor with excellent luminescence properties. From perspective of practical application, the research on $LaPO_4$:Ce,Tb phosphor by co-precipitation method has been highlighted because of easiness of chemical homogeneity using co-precipitation method. And, it is confirmed that a regular morphology and non-agglomerated particles are helpful for forming a densely packing phosphor layer and extending lamp life [6, 17]. So, many efforts have been paid to prepare $LaPO_4$:Ce,Tb phosphor with a regular morphology and non-agglomerated particles [3, 6, 8, 18]. In particular, a micron-sized quasi-spherical or a micron-sized spherical particle was supposed as the most favorable one [17, 27]. However, it is difficult to prepare micron-sized spherical $LaPO_4$:Ce,Tb particles by co-precipitation method though some $LaPO_4$:Ce,Tb particles with different morphologies, such as the micron-sized quasi-spherical particles [17], nano-wires [22], nano-spherical particles [23], nano-leaves [24], hexagonal prism particle [25] and spindle-shape particle [26], have been successfully fabricated by co-precipitation method.

In this work, we present a new homogeneous precipitation method by which the micron-sized spherical $LaPO_4$:Ce,Tb particles were synthesized. Firstly, micron-sized spherical $LaPO_4$:Ce,Tb precipitate was prepared. And then, the corresponding micron-sized spherical $LaPO_4$:Ce,Tb phosphor was fabricated. Furthermore, the growth mechanism of micron-sized spherical precipitates was investigated.

2. Experimental

In order to tell the differences between spherical $LaPO_4$:Ce,Tb phosphor and conventional $LaPO_4$:Ce,Tb phosphor. A conventional co-precipitation method was employed to prepare irregular $LaPO_4$:Ce,Tb phosphor as mentioned in previous reports [17, 19]. Figure 1 shows the sketch map of synthesizing $LaPO_4$:Ce,Tb phosphor by two different methods.

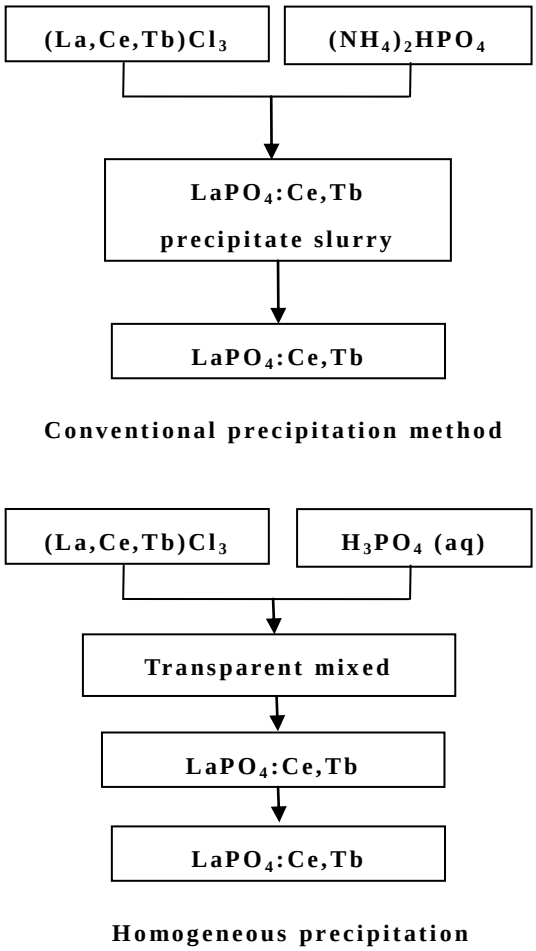

Fig. 1. The sketch map of different synthesis methods for LaPO4:Ce,Tb phosphors.

La_2O_3 (99.99%), $Ce_2(CO_3)_3$ (99.9%), Tb_4O_7 (99.99%), HCl (A.R.), H_3PO_4 (A.R.) and $(NH_4)_2HPO_4$ (A.R.) were used as starting materials. $LaCl_3$, $CeCl_3$ and $TbCl_3$ solution were obtained by dissolving La_2O_3, $Ce_2(CO_3)_3$ and Tb_4O_7 using HCl, respectively. And then, the rare earth chlorination solutions were mixed at a molar ratio of La/Ce/Tb = 0.55:0.30:0.15. The mixed rare earth chlorination solution is diluted to 1.0 mol L^{-1}. $(NH_4)_2HPO_4$ was dissolved in distilled water to obtain a $(NH_4)_2HPO_4$ solution of 1.05 mol L^{-1}. H_3PO_4 was diluted into a H_3PO_4 solution of 0.525 mol L^{-1}.

Conventional method: The rare earths chlorination solution and equal amount of $(NH_4)_2HPO_4$ solution were simultaneously fed into a beaker which contained a certain amount of distilled water at ambient temperature. The $LaPO_4$:Ce,Tb precipitate was produced at once. The pH value was kept in a range of 2.0–3.0 by adding HCl acid into the beaker. And then, the precipitate slurry was ripening at 80 °C for 3 h. Finally, the precipitate slurry was washed using distilled water and dried at 120 °C. The as-prepared $LaPO_4$:Ce,Tb precipitate was designated as LAP-A. The corresponding $LaPO_4$:Ce,Tb phosphor was fabricated by firing in a reducing atmosphere at 1000 °C for 3 h and was denoted as the LAP-A′.

Homogeneous Method: A 400 ml H_3PO_4 solution of 0.525 mol L^{-1} was mixed with 200 ml rare earths chlorination solution of 1.0 mol L^{-1} in a 1000 ml beaker at ambient temperature (a slight excess amount of PO_4^{3+}). Due to high acid, the mixed solution kept clear at ambient temperature. And then, the mixed solution was heated by 95 °C in a water-bath. The $LaPO_4$:Ce,Tb precipitate was produced when the temperature of mixed solution was rising. Then, the precipitate slurry was ripening at 95 °C for 3 h in a mixed soluion of 1.0 mol L^{-1} HCl acid and about 0.017 mol L^{-1} H_3PO_4 acid. Finally, the precipitate slurry was washed using distilled water and dried at 120 °C. The as-prepared $LaPO_4$:Ce,Tb precipitate was denoted as LAP-B. The corresponding $LaPO_4$:Ce,Tb phosphor was fabricated by firing in a reducing atmosphere at 1000 °C for 3 h and was designated as the LAP-B′.

Powder X-ray diffraction (XRD, Philips, X' pert TRO MPD) using Cu Kα radiation at 40 kV/25 mA at 0.06° s^{-1} was employed to characterize the crystal phase of samples. Scanning electron microscopy (SEM, Philips-XL30W/TMP) was conducted to check the particle shape and size. Photoluminescence excitation (PLE) and emission (PL) spectra were recorded using a Hitachi F-4700 fluorescence spectrophotometer.

3. Results and discussion

The TG-DTA characteristic of as-prepared $LaPO_4$:Ce,Tb precipitates synthesized by different methods is illustrated in Figure 2. Both samples display similar profiles of TG-DTA. Two endothermic peaks around 95 °C and 240 °C are observed in both DTA curves. Meanwhile, a weight loss of about 7.0 % is shown in both TG curves, which is associated with the loss of residual water. The weight losses slow down when the temperature rises from 240 °C to 1200 °C. However, there are two endothermic peaks above 1000 °C in the DTA curve of LAP-B precursor. The reason remains unclear due to no endothermic peak above 1000 °C in the DTA curve of LAP-A precursor.

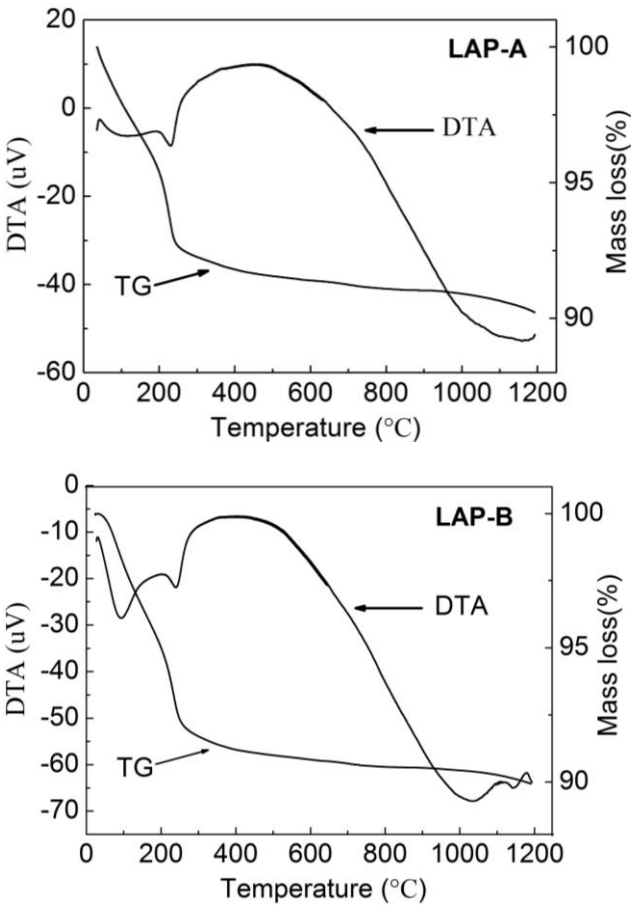

Fig. 2. TG-DTA profiles for $LaPO_4$:Ce,Tb precipitates prepared by different methods.

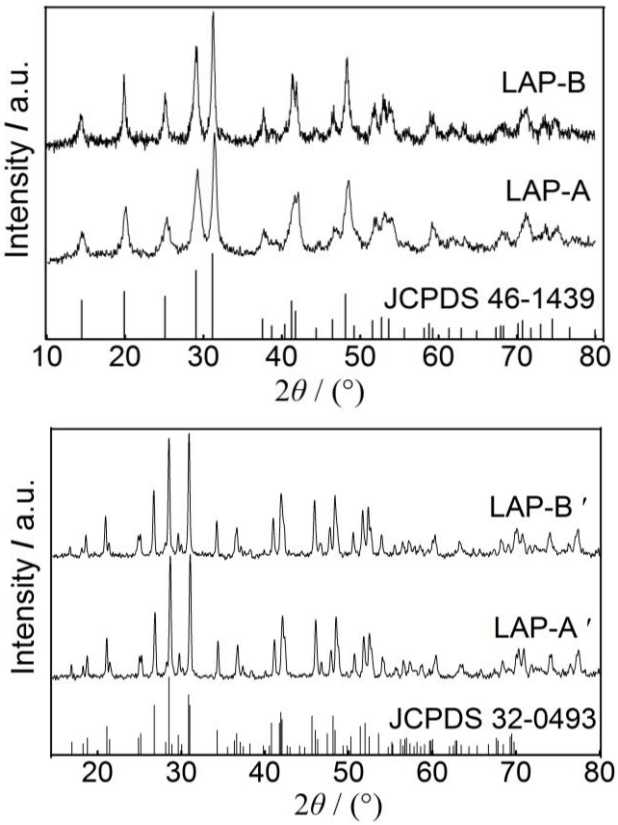

Fig. 3. XRD patterns of the $LaPO_4$:Ce,Tb precipitates and phosphors prepared by different methods.

Fig. 3 shows the patterns of $LaPO_4$:Ce,Tb precipitates and phosphors. The XRD patterns of LAP-A and LAP-B precursors can be indexed as $LaPO_4 \cdot 0.5H_2O$ with rahabodophane structure corresponding to JCPDS file (no. 46-1439), which is in agreement with the results in previous literature [11]. The peaks intensity of LAP-B precursor is slightly stronger than that of LAP-A precursor, which is attributed to a better crystallinity of LAP-B precursor at a higher ripening temperature. There is no difference between XRD patterns of LAP-A′ and LAP-B′phosphors. The XRD patterns of LAP-A′ and LAP-B′ phosphors are in agreement with that of the JCPDS file (no. 32-0493), which can be indexed as $LaPO_4$ with monazite structure [9, 17, 25].

Fig. 4 shows SEM micrographs of $LaPO_4$:Ce,Tb precipitates and phosphors. The intensive agglomerated particles consisting of string-shape primary nano-particles are observed in SEM image of LAP-A precursor prepared by the conventional method. LAP-A′ phosphor particles remain agglomerated morphology of LAP-A precursor particles. In addition, compared to LAP-A precursor particles, LAP-A′ phosphor particles display a smoother surface. In all, the morphology of LAP-A′phosphor particles is similar to that of $LaPO_4$:Ce,Tb phosphor particles in the literature [19]. In contrast to the LAP-A precursor, the LAP-B precursor demonstrates utterly different morphology. The spherical particles with a few extent of agglomeration are shown in SEM image of LAP-B precursor prepared by the homogeneous precipitation method. The diameters of LAP-B precursor particles are in the range of 2–5 μm. Except for a smoother surface of particles, the LAP-B′ phosphor illustrates the similar morphology of LAP-B precursor.

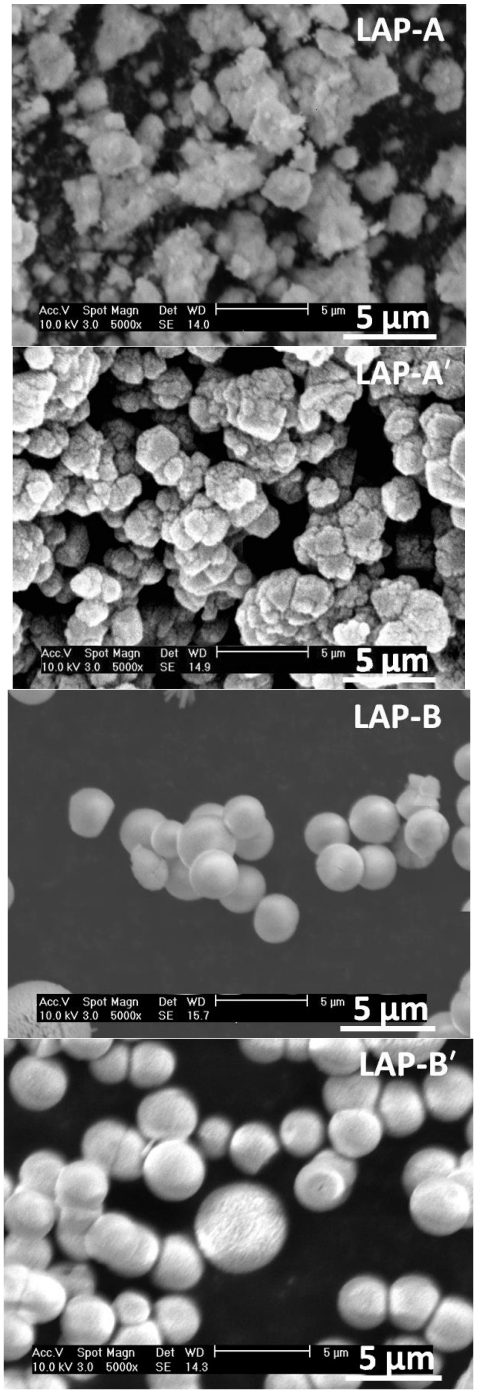

Fig. 4. SEM micrographs of $LaPO_4$:Ce,Tb precipitates and phosphors prepared by different methods.

In order to figure out the growth mechanism of spherical precipitate, three $LaPO_4$:Ce,Tb precipitate samples were prepared under different conditions as following: 1) In the process of homogeneous precipitation reaction, the transparent mixed solution was continuously stirring when the temperature of the mixed solution was rising. 2) In the process of homogeneous precipitation reaction, the transparent mixed solution suffered a slight stir every 10 minutes when the temperature of the mixed solution was rising. 3) In the process of homogeneous precipitation reaction, the transparent mixed solution was kept still when the temperature of the mixed solution was rising. These three samples were denoted as LAP-B1, LAP-B2 and LAP-B3, respectively. Fig. 5 shows the SEM micrographs of $LaPO_4$:Ce,Tb precipitates LAP-B1, LAP-B2 and LAP-B3. LAP-B1 displays the irregular secondary particles consisting of needle-shape primary particles. LAP-B2 precursor demonstrates a combination of the semi-spherical and spherical secondary particles. LAP-B3 shows the spherical secondary particles. Obviously, the homogeneous precipitation reaction includes two steps: 1) the formation of needle-shape primary particle, 2) the formation of agglomerated particles. The primary particles tend to form spherical agglomerated particle due to low surface energy of spherical particle. So, the spherical secondary particles can be achieved when the transparent mixed solution was kept still.

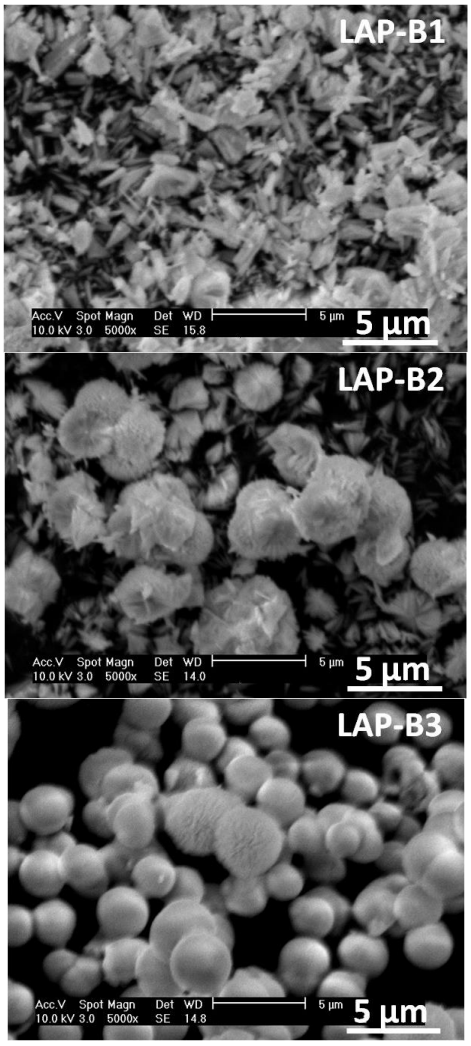

Fig. 5. SEM micrographs of $LaPO_4$:Ce,Tb precipitates prepared under different conditions by a homogeneous precipitation method.

Fig. 6 shows excitation (a) and emission (b) spectra of $LaPO_4$:Ce,Tb phosphors prepared by different methods. The excitation spectra were recorded using an emission wavelength of 545 nm. The emission spectra were collected using an excitation wavelength of 276 nm. In agreement with the previous report [25], the excitation spectra consist of a broad band in the range 220−300 nm and several small peaks in the range of 340−380 nm. The broad band is due to 4f→5d electronic transitions of Ce^{3+}. The small peaks are attributed to 4f→4f electronic transitions of Tb^{3+}. The emission spectra contain a broad weak emission band in the range of 300−400 nm and four strong green emission peaks [12, 13, 15]. The broad weak emission band is associated with the Ce^{3+}. The four peaks at 489 nm, 545 nm, 586 nm and 622 nm are ascribed to the ($^5D_4$-$^7F_6$), ($^5D_4$-$^7F_5$), ($^5D_4$-$^7F_4$) and ($^5D_4$-$^7F_3$) transitions of Tb^{3+} [25]. The weak emission band of Ce^{3+} and strong emission peaks of Tb^{3+} indicate a high efficiency of energy transition from Ce^{3+} to Tb^{3+}. LAP-A′ and LAP-B′ phosphors show a simlilar intensity of Ce^{3+} emission. However, the LAP-B′ phosphor displays a stronger intensity of green emission than LAP-A′ phosphor. The stronger emission intensity of LAP-B′ phosphor is mainly attributed a smooth surface of particles because defect concentration are much diminished at the smoother surface, as reported in previous literatures [3, 22].

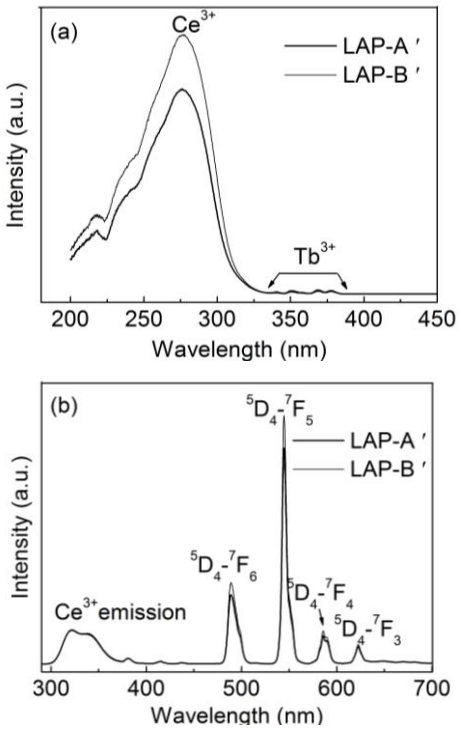

Fig. 6. Excitation (a, $\lambda_{emission}$ = 454 nm) and emission (b, $\lambda_{excitation}$ = 276 nm) spectra of $LaPO_4$:Ce,Tb phosphors prepared by different methods.

4. Conclusions

In summary, the micro-sized spherical $LaPO_4$:Ce,Tb precipitate can be fabricated via the homogeneous precipitation method by which the secondary particle can be formed in a process of a self-assembly of the needle-shape primary particles. And, the corresponding $LaPO_4$:Ce,Tb phosphor possesses the similar morphology of $LaPO_4$:Ce,Tb precipitate. The as-prepared spherical $LaPO_4$:Ce,Tb phosphor particles demonstrate a higher brightness than irregular particles prepared by a conventional co-precipitation method.

Reference

[1] M. Z. Su, J. Zhou, K. S. Shao, J. Alloys Compd. **207–208**, 406 (1994).
[2] J. H. Lin, G. Q. Yao, Y. Dong, B. Park, M .Z. Su, J. Alloys Compd. **225**, 124 (1995).
[3] Z. X. Fu, W. B. Bu, Solid State Sci. **10**, 1062 (2008).
[4] H. L. Zhu, E. Z. Zhu, H. Yang, L. N. Wang, D. L. Jin, K. H. Yao, J. Am. Ceram. Soc. **91**, 1682 (2008).
[5] I. W. Lenggoro, B. Xia, H. Mizushima, K. Okuyama, N. Kijima, Materials Letters **50**, 92 (2001).
[6] Y. C. Kang, E. J. Kim, D. Y. Lee, H. D. Park, J. Alloys Compd. **347**, 266 (2002).
[7] T. Jin, S. Tsutsumi, Y. Deguchi, K. Machida, G. Adachi, J. Alloys Compd. **252**, 59 (1997).
[8] H. Meyssamy, K. Riwotzki, A. Kornowski, S. Naused, M. Haase, Adv. Mater. **11**, 840 (1999).
[9] W. S. Song, H. N. Choi, Y. S. Kim, H. Yang, J. Mater. Chem. **20**, 6929 (2010).
[10] S. Erdei, F. W. Ainger, D. Ravichandran, W. B. White, L. E. Cross, Mater. Lett. **30**, 389 (1997).
[11] V. Buissette, M. Moreau, T. Gacoin, J. P. Boilot, J. Y. Chane-Ching, T. L. Mercier, Chem. Mater. **16**, 3767 (2004).
[12] K. Riwotzki, H. Meyssamy, H. Schnablegger, A. Kornowski, M. Haase, Angew. Chem. Int. Ed. **40**, 573 (2001).
[13] X. X. Zhu, Q. H. Zhang, Y. G. Li, H. Z. Wang, J. Mater. Chem. **20**, 1766 (2010).
[14] G. Buhler, C. Feldmann, Angew. Chem. Int. Ed. **45**, 4864 (2006).
[15] A. Zharkouskaya, C. Feldmann, K. Trampert, W. Heering, U. Lemmer, Eur. J. Org. Chem. 873 (2008).
[16] V. Pankratov, A. I. Popov, A. Kotlov, C. Feldmann, Opt. Mater. **33**, 1102 (2011).
[17] X. F. Hu, S. R. Yan, L. Ma, G. J. Wan, J. G. Hu, Powder Technol. **192**, 27 (2009).
[18] F. Duault, M. Junker, P. Grosseau, B. Guilhot, P.

Iacconi, B. Moine, Powder Technol. **154**, 132 (2005).
[19] Z. Q. Long, L. Ren, Z. W. Zhu, D. L. Cui, N. Zhao, M. L. Li, M. S. Cui, X. W. Huang, J. Rare Earth **24**, 137 (2006).
[20] Z. Wu, T. Jiang, N. X. Liang, Y. L. Sun, L. M. Dong, Appl. Mech. Mater. **274**, 467 (2013).
[21] Y. X. Yang, C. Li, S. L. Yuan, B. Fang, G. R. Chen, Ceram. Silik. **49**, 63 (2005).
[22] M. Yang, H. P. You, K. Liu, Y. H. Zheng, N. Guo, H. J. Zhang, Inorg. Chem. **49**, 4996 (2010).
[23] N. O. Nuñez, S. R. Liviano, M. Ocaña, J. Colloid Interface Sci. **349**, 484 (2010).
[24] A. K. Gulnar, V. Sudarsan, R. K. Vatsa, R. C. Hubli, U. K. Gautam, A. Vinu, A. K. Tyagi, Cryst. Growth Des. **9**, 2451 (2009).
[25] Y. R. Shi, Y. H. Wang, D. Wang, B. T. Liu, Y. H. Li, L. Wei, Cryst. Growth Des. **12**, 1785 (2012).
[26] S. Rodriguez-Liviano, F. J. Aparicio, A. I. Becerro, J. Garcı´a-Sevillano, E. Cantelar, S. Rivera, Y. Herna´ndez, J. M. de la Fuente, M. Ocan˜a, J. Nanopart. Res. **15**, 1402 (2013).
[27] S. Oshio, K. Kitamura, T. Shigeta, S. Horii, T. Matsuoka, S. Tanaka, H. Kobayashi, J. Electrochem. Soc. **146**, 392 (1999).

*Corresponding author: slm@scetc.net